

# Extremely rapid star cluster disruption in high-shear circumnuclear starburst rings: the unusual case of NGC 7742

Richard de Grijs<sup>1,2</sup> and Peter Anders<sup>1</sup>

## ABSTRACT

All known mass distributions of recently formed star cluster populations resemble a ‘universal’ power-law function. Here we assess the impact of the extremely disruptive environment in NGC 7742’s circumnuclear starburst ring on the early evolution of the galaxy’s high-mass ( $\sim 10^5$ – $10^7 M_\odot$ ) star cluster population. Surprisingly, and contrary to expectations, at all ages – including the youngest,  $\lesssim 15$  Myr – the cluster mass functions are robustly and verifiably represented by lognormal distributions that resemble those commonly found only for old, evolved globular cluster systems in the local Universe. This suggests that the high-shear conditions in the NGC 7742 starburst ring may significantly speed up dynamical star cluster destruction. This enhanced mass-dependent disruption rate at very young ages might be caused by a combination of the starburst ring’s high density and the shear caused by the counterrotating gas disk in the galaxy’s inner region.

*Subject headings:* galaxies: evolution — galaxies: individual (NGC 7742) — galaxies: starburst — galaxies: star clusters: general

## 1. Introduction

Circumnuclear rings in spiral galaxies represent environmental conditions that are conducive to intense star and star cluster formation. Since the early work by Sérsic & Pastoriza (1965, 1967), many intensely star-forming rings featuring compact ‘hot spots’ have been identified, while high spatial resolution *Hubble Space Telescope* (*HST*) observations have revealed the presence of numerous young (a few  $\times 10^7$  yr) and intermediate-age (up to a few Gyr) star clusters in these structures (e.g., Barth et al. 1995; Maoz et al. 1996, 2001; Ho

---

<sup>1</sup>Kavli Institute for Astronomy and Astrophysics, Peking University, Yi He Yuan Lu 5, Hai Dian District, Beijing 100871, China; grijs@pku.edu.cn, anders@pku.edu.cn

<sup>2</sup>2012 Selby Fellow, Australian Academy of Science

1997; Buta et al. 2000; de Grijs et al. 2003; Mazzuca et al. 2008; van de Ven & Chang 2009; Hsieh et al. 2012).

NGC 7742, an almost face-on, SA(r)b-type spiral galaxy at a distance  $D = 22.2$  Mpc ( $1'' \equiv 107$  pc) that features a  $\sim 2$  kpc-diameter circumnuclear ring, is an unusual example of this class of galaxies, however: it does not have a dominant bar (but see Laine et al. 2002; Comerón et al. 2008). Sil’chenko & Moiseev (2006) obtained two-dimensional kinematic data (a combination of integral-field and long-slit spectroscopy) and deep optical imaging of the galaxy. They interpreted the presence of a *global* gaseous subsystem that is counterrotating with respect to the *global* disk-like rotation of the stars, combined with the starburst ring, as the result of a past minor merger with a gas-rich dwarf galaxy (see also Mazzuca et al. 2006; Tutukov & Fedorova 2006). The non-axisymmetric gravitational perturbations resulting from such a merger are similar to those associated with a bar. Both types of perturbations can result in a torque change at a particular radius and, hence, accumulation of gas into a circumnuclear ring.

Here we explore the mass distribution of the young star clusters associated with the galaxy’s starburst ring. Our aim is to assess the impact of the ring’s high-shear conditions on the formation and early evolution of this star cluster population.

## 2. Observations and data reduction

We obtained high-resolution images of NGC 7742 from the *HST* Data Archive. The galaxy was observed with the Wide-Field and Planetary Camera/2 (WFPC2) in the F336W, F555W, F675, and F814W filters with exposure times of 4200, 960, 960, and 1360 s, respectively, as part of proposal GO-6276 (PI Westphal). The galaxy’s center and its circumnuclear ring were centered on the WF3 chip ( $0.1''$  pixel $^{-1}$ ); all four exposures were aligned to subpixel accuracy (neither image rotation nor scaling was required). Although we also explored the use of a near-infrared F160W image obtained with the Near-Infrared Camera and Multi-Object Spectrometer (NICMOS), the field of view sampled and the signal-to-noise ratio (S/N) – combined with the smoother distribution of old stellar populations traced by near-infrared light compared to young star-forming regions – proved insufficient.

### 2.1. Basic reduction

Our data reduction followed the detailed description and justification in de Grijs et al. (2012), which we briefly summarize here. The standard deviations ( $\sigma_{\text{sky}}$ ) of the numbers

of counts in empty sections in all images were established to ascertain a ‘sky’ background count for each filter. We used multiples of this background count as thresholds above which the numbers of source detections in both the F555W and F814W filters were calculated. The number of detections initially decreases rapidly with increasing detection threshold. This indicates that our ‘source’ detections are noise-dominated in the low-threshold regime. Where the rapid decline flattens off, the detections become dominated by ‘real’ objects, either cluster candidates or background-intensity variations. In view of the images’ individual S/N characteristics, the most suitable thresholds, at  $4$  and  $3\sigma_{\text{sky}}$ , were  $0.067$  and  $0.061$  counts  $\text{s}^{-1}$  (917 and 764 sources) for the F555W and F814W filters, respectively.

We subsequently employed a cross-identification procedure to select the 398 sources that coincided with intensity peaks within 1.4 pixels of each other in the F555W $\otimes$ F814W filter combination (i.e., allowing for 1-pixel mismatches in both spatial directions). Next, we applied a Gauss-fitting routine to each candidate cluster. Although we do not expect to detect individual stars at the distance of NGC 7742, size selection can help us to remove unlikely cluster candidates. We generated model WF3 point-spread functions (PSFs) using TINYTIM (Krist & Hook 2001) and applied a conservative clipping approach to weed out source detections characterized by Gaussian widths in the F555W image,  $\sigma_{\text{F555W}}$ , that were too small to be ‘real’ point sources (i.e.,  $\sigma_{\text{F555W}} \leq 0.8$  pix), such as cosmic rays or detector artefacts. This left us with a sample containing 352 sources. The resulting size distribution exhibits a clear peak near the PSF size (with  $\sim 80\%$  of the clusters characterized by  $\sigma_{\text{F555W}} \lesssim 2$  pixels  $\simeq 22$  pc), with a shallow tail toward more extended objects. We checked that the five most extended objects ( $4 \leq \sigma_{\text{F555W}} \leq 9$  pixels, or  $\sigma_{\text{F555W}} \lesssim 100$  pc) are associated with clear star-forming complexes. They are unlikely background galaxies, but they might be cluster complexes or cluster mergers (e.g., Fellhauer & Kroupa 2005; Brüns et al. 2011).

## 2.2. Photometry

Our custom-written IDL aperture-photometry task employs source radii and sky annuli *individualized* for each cluster candidate. We used a source aperture radius of  $3 \times \sigma_{\text{F555W}}$ , and  $3.5$  and  $5 \times \sigma_{\text{F555W}}$  for the inner and outer sky annuli, respectively. This was based on inspection of the stellar growth curves, to identify where the object profiles disappear into the background noise. We verified that our source radii were chosen conservatively and sufficiently far out so as not to exclude any genuine source flux. We also checked that the background annuli were chosen appropriately and not dominated by neighboring sources. Our observations are characterized by a 50% completeness limit at  $m_{\text{F555W}} = 23.0$  (ST) mag for the galaxy as a whole and  $m_{\text{F555W}} = 22.0$  mag in the starburst ring. Following common

practice, we quote our completeness limit in the  $V$ -band filter. However, our analysis is limited by the F336W image, which has the lowest S/N. The corresponding limits are  $m_{\text{F336W}} = 22.5$  and 21.5 mag, respectively.

As a final step, we removed objects that lacked a robustly determined flux in one or more filters: we need a minimum of four filters to determine reliable cluster parameters (Anders et al. 2004). Our final sample contained 317 objects. Three quarters of the sources rejected in this final step lacked reliable photometry in the F336W filter.

### 3. Cluster ages and masses

#### 3.1. Models

For our cluster age and mass determinations, we adopted the set of GALEV simple stellar population (SSP) models (Kotulla et al. 2009; and references therein) assuming solar metallicity, based on the good match of previous NGC 7742 analyses to solar-metallicity models (Mazzuca et al. 2006; Peletier et al. 2007; Sarzi et al. 2007). For a given cluster, we used the ANALYSED tools (Anders et al. 2004) to compare the shape of the observed spectral-energy distribution (SED) with the shapes of GALEV model SEDs (as a function of age and foreground extinction). The associated cluster mass was derived from the magnitude offset between the observed and model SEDs. Each model SED (and its associated physical parameters) was assigned a probability based on the  $\chi^2$  value of this comparison. The model data set with the highest probability was adopted as the most representative set of parameters. Models with decreasing probabilities were summed up until a 68.26% ( $1\sigma$ ) total probability was reached, to estimate the uncertainties in the best-fitting model. These uncertainties are upper limits, since their determination specifically also takes into account effects such as the presence of several local minima for a given cluster (e.g., owing to the age–metallicity degeneracy) and discretization in parameter space.

Fig. 1, shows the derived ages and masses for our 317 cluster candidates. The solid line represents the expected evolution of an SSP for  $m_{\text{F555W}} = 23.0$  mag. The 256 starburst ring clusters are indicated as circled crosses. We consider clusters to be part of the ring if they are located at radii,  $R$ , of  $0.52 \leq R \leq 1.35$  kpc. Adopting the more conservative range of  $0.72 \leq R \leq 1.35$  (Mazzuca et al. 2008) would remove only seven objects from our sample.

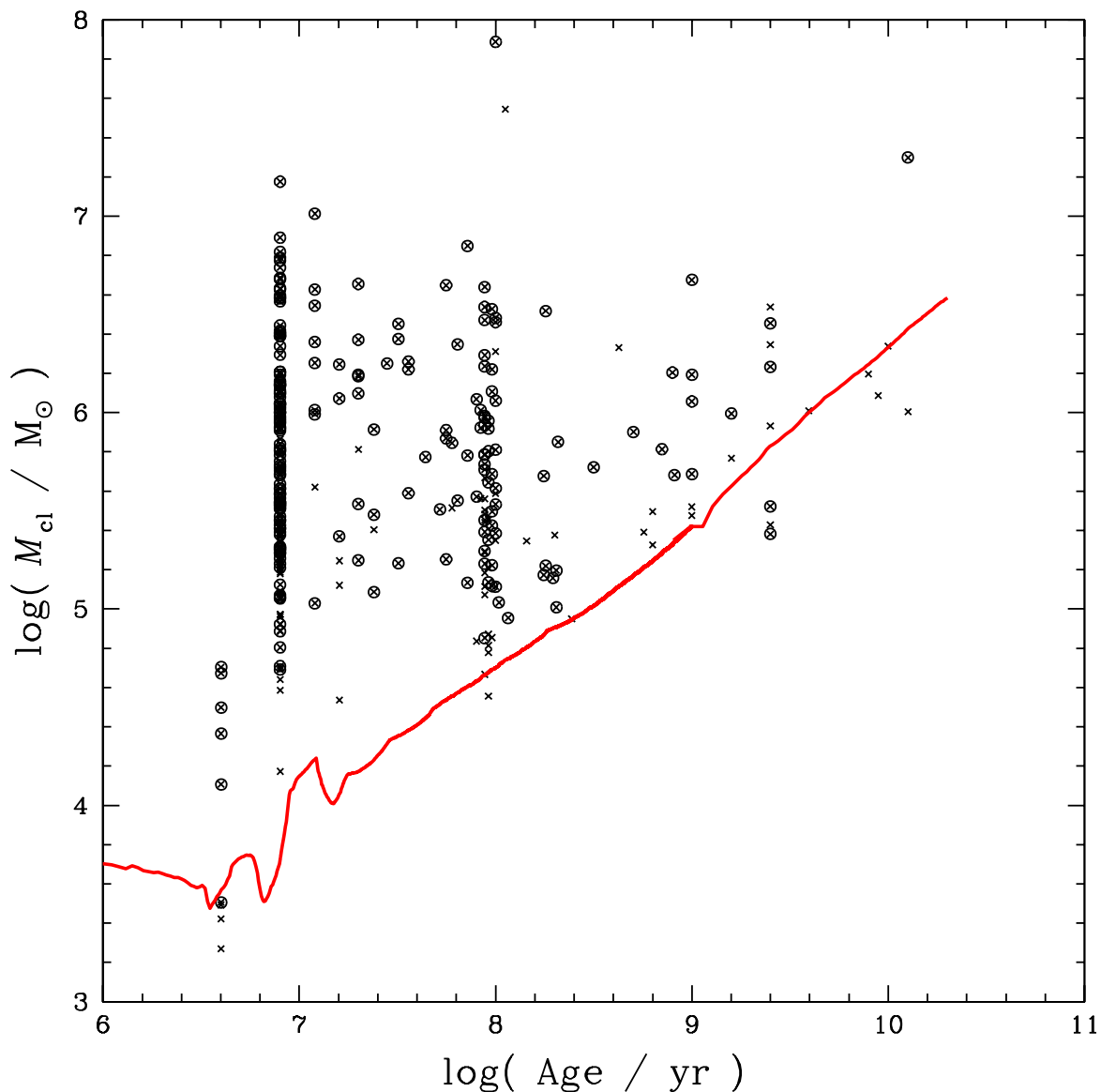


Fig. 1.— The NGC 7742 star cluster population in the diagnostic age–mass plane. Error bars have been omitted for reasons of clarity (see text for a discussion of their impact). The solid line represents SSP evolution at our 50% completeness limit, adopting  $m_{F555W} = 23.0$  mag. Circled crosses: starburst ring clusters.

### 3.2. Age distribution

Fig. 1 indicates that most clusters have ages of either around 10 or 100 Myr, but this result is caused by the effects of discretization. It is well-known that age estimates based on broad-band imaging observations tend to be narrowly confined to ‘chimneys’ associated with local minima in parameter space; the effects of interpolating discrete isochrones for cluster age determinations and the resulting artifacts in age-mass space were discussed in depth by Bastian et al. (2005) and Gieles et al. (2005). The chimney near 10 Myr corresponds to the appearance of red supergiants in stellar populations, while 100 Myr is the age at which asymptotic giant branch stars first show up.

The majority of clusters in the starburst ring are found in either one of the two chimneys, roughly in a 2:1 ratio between the younger and older chimneys. They are generally well mixed along the ring, although a handful of clusters younger than 10 Myr is found in the northern and northeastern sections of the ring. This behavior is expected given that stars and gas tend to circulate along such structures in typically a few  $\times 10^7$  yr (cf. Sarzi et al. 2007). Although the stellar age map of Peletier et al. (2007) does not provide us with sufficient spatial information to assess the validity of our results, they state that the ring is composed of young stellar populations (see also Sarzi et al. 2007). Mazzuca et al.’s (2008) age distribution of 38 HII regions shows qualitatively similar trends as deduced here.

### 3.3. Masses and mass functions

Approximately 95% of our sample clusters have derived masses  $\gtrsim 10^5 M_\odot$ . Based on our recent analysis of the impact of stochastic sampling of stellar mass functions (MFs) on integrated star cluster properties (de Grijs et al. 2012; see also Silva-Villa & Larsen 2011) we conclude that the effects of stochasticity are minimal in the mass range covered by the NGC 7742 clusters. In de Grijs et al. (2005), we concluded that application of the ANALYSED approach based on the GALEV models led to high-accuracy relative mass determinations within a given cluster system (Anders et al. 2004). We found that the accuracy with which the cluster mass distribution can be reproduced using different approaches (including different SSP models, filter combinations, and input physics) is  $\sigma_M = \Delta \langle \log(M_{cl}/M_\odot) \rangle \leq 0.14$ . In fact, we concluded that “[t]his implies that mass determinations are mostly insensitive to the approach adopted.” This is so, because the mass-to-light ratio of a given SSP depends only weakly on the population’s age.

Since the detection limit of our star clusters is a function of their age, we need to carefully select the age and mass ranges over which to compare the cluster population’s evolution. In

Fig. 2 we compare the MFs of the clusters in the ring as a function of age. The error bars represent Poissonian uncertainties. We focus specifically on the two dominant age ranges, i.e.,  $6.8 \leq \log(t/\text{yr}) \leq 7.2$  and  $7.8 \leq \log(t/\text{yr}) \leq 8.2$ . The corresponding mass ranges that are affected by negligible or only limited sample incompleteness (up to 50%) for these two age bins are  $\log(M_{\text{cl}}/M_{\odot}) \geq 4.0$  and 4.5, respectively, where we have corrected our analysis for the effects of up to 50% incomplete sampling. (We also show the MFs of the galaxy’s entire cluster population in the relevant age ranges as black open circles for comparison.) Given the extremely young age range of the youngest selection, it is surprising that the cluster MFs resemble a lognormal distribution in mass. To verify that this is a robust result, we confirmed that the cluster MF in the age range between both chimneys exhibits a similar behavior.

#### 4. Implications and Concluding Remarks

It is now well established that cluster MFs at the time of star (cluster) formation are well described by power-law distributions of the form  $dN/dM_{\text{cl}} \propto M_{\text{cl}}^{-\alpha}$ , where  $\alpha$  is usually close to 2 (cf. de Grijs et al. 2003; Portegies Zwart et al. 2010; Fall & Chandar 2012). This power-law form seems ubiquitous and independent of initial stellar or gas density: it is found in environments ranging from the low-density, quiescent Magellanic Clouds (de Grijs & Anders 2006; de Grijs & Goodwin 2008) to the high-density, violently interacting Antennae galaxies (e.g., Whitmore et al. 2010). An initial power-law MF seems, therefore, a reasonable boundary condition for our discussion of Fig. 2.

If we assume, not unreasonably given the long timescales involved, that the highest-mass clusters in NGC 7742 essentially represent their formation conditions, we can approximate the high-mass end of the MFs by a power law with a slope of  $-2$  (see the dashed lines in Fig. 2). The approximately lognormal MF shapes imply that a large fraction of the lower-mass clusters are ‘missing’ compared to expectations. Based on our current best understanding of the early evolution of cluster MFs, it is particularly surprising that the cluster MF in the youngest age bin resembles a lognormal distribution (in fact, a power-law mass function is generally a poor fit, even for the highest masses of  $M_{\text{cl}} \gtrsim 10^6 M_{\odot}$ ). Except if we release the assumption that the initial cluster MF was a power law – which would contradict most observational studies in this very active area of current research – three effects could have caused this discrepancy: (i) technical issues related to our age and mass determinations, (ii) evolution of the star cluster population on very short timescales ( $\lesssim 10^7$  yr), and/or (iii) differences in the cluster formation conditions compared to other environments featuring large samples of young star clusters. Note that issues related to sample incompleteness

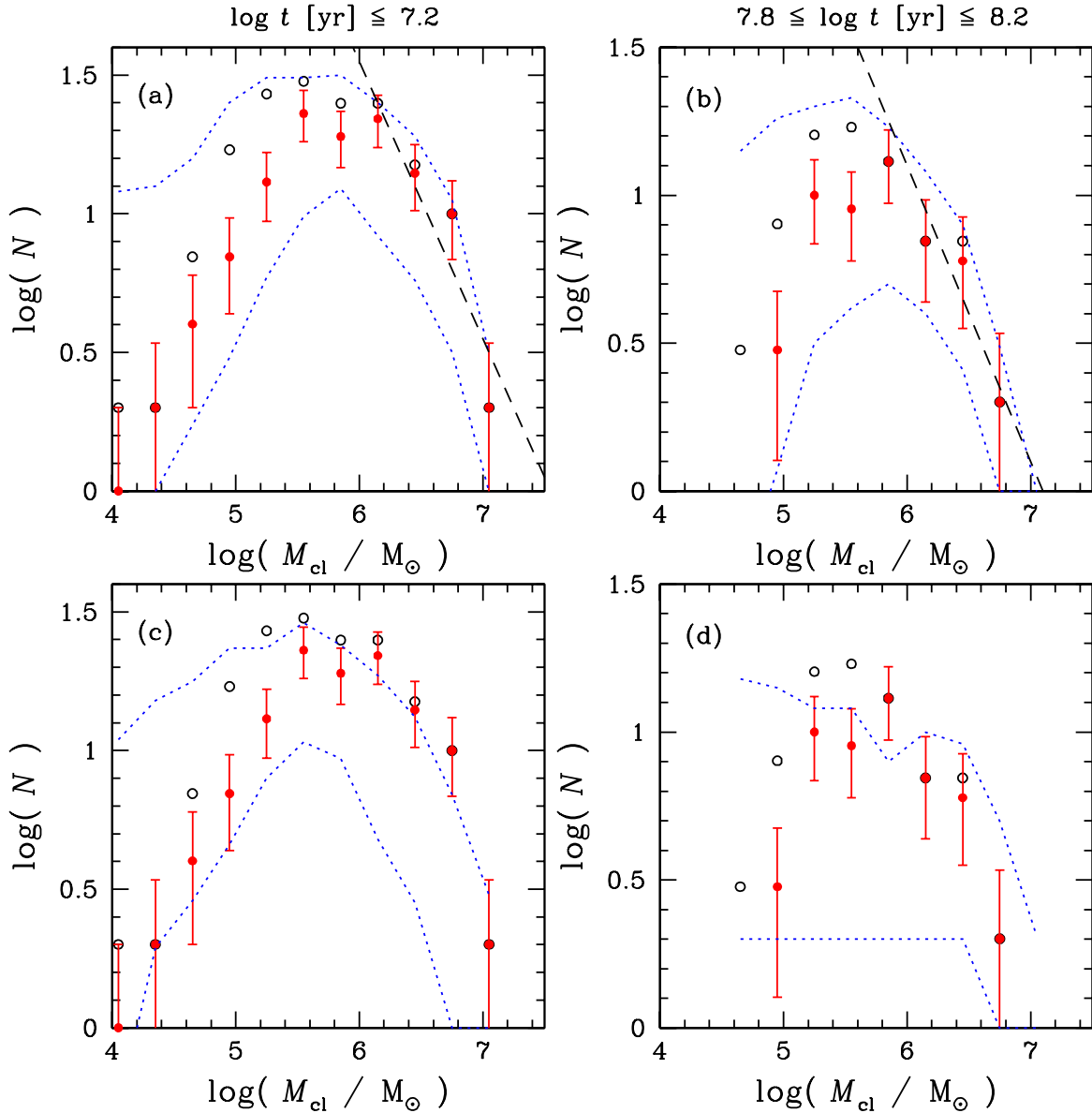


Fig. 2.— NGC 7742 cluster MFs and their Poissonian uncertainties for ages  $t$  of  $\log(t/\text{yr}) \leq 7.2$  (left-hand panels) and  $7.8 \leq \log(t/\text{yr}) \leq 8.2$  (right-hand panels) and for all clusters in the galaxy above our 50% completeness limit (corrected for incompleteness). Red solid bullets: Clusters in the starburst ring; black open circles: MFs of the full, galaxy-wide cluster populations. The blue dotted lines indicate the upper and lower envelopes of the ring-cluster MFs based on two statistical redeterminations of the cluster ages and masses (top panels: Gaussian error distribution; bottom panels: uniform uncertainties; see §4). The dashed lines represent the expected power-law mass distributions with an index of  $\alpha = 2$ .



will only affect the lowest cluster masses in our completeness-corrected samples, i.e., masses *significantly below* the observed peaks of the MFs.

To ascertain whether the observed ‘turnover’ in the NGC 7742 cluster MF could have been caused by artefacts related to our fitting approach, we performed two statistical tests. For each of our sample clusters we considered the original age determination and its  $1\sigma$  uncertainties. We then randomly drew a new age from within this uncertainty range and – using the observed fluxes – redetermined its mass based on the appropriate, age-dependent mass-to-light ratio provided by our SSP models. We redetermined the cluster mass 1000 times using two different probability distributions in age. The first adopted the highest probability given by the original age determination and with a (skewed) Gaussian probability distribution of which the width and rate of decrease were determined by the original error bars (blue dotted envelopes in Fig. 2, top panels). Our second test was based on a uniform probability distribution within the error range determined for the original age estimate (Fig. 2, bottom panels). Our random resampling of the cluster ages and the subsequent redetermination of their masses firmly rules out an original power-law MF. This implies that the derived MF shape is robust with respect to artefacts introduced by our fitting approach. (Note that the systematic offset in mass for the resampling test based on a uniform probability distribution reflects the systematically larger uncertainty ranges toward older ages compared to the error bars toward younger ages.)

It thus appears that at least part of the observed ‘downturn’ toward lower masses may be due to either the effects of star cluster evolution or their formation conditions. From an evolutionary perspective, the conditions in the galaxy’s starburst ring appear to speed up the destruction or evaporation of a large fraction of the lower-mass clusters. We speculate that this enhanced cluster disruption rate at very young ages is caused by a combination of the high stellar and gas density in the starburst ring<sup>1</sup> and the shear caused by the galaxy-wide counterrotating gas disk. Although the gas and stellar disks rotate in opposite senses globally, the high gas density and filling factor (cf. Falcón-Barroso et al. 2006) and our detection of very young clusters in the ring (which presumably formed *in situ* and are hence expected to co-rotate with the gaseous subsystem) may have led to increased shear, as well as star/gas and star (cluster)/star (cluster) interactions in the ring. In addition, at the ring’s galactocentric radius, the galaxy’s rotation curve has already reached its constant level (Sil’chenko & Moiseev 2006), so that differential rotation across the ring will induce

---

<sup>1</sup>If we adopt Mazzuca et al.’s (2008) ring size and assume that the ring thickness follows that of generic, late-type galactic disks, with a ratio of scale length to scale height of order eight (e.g., de Grijs 1998), we obtain an approximate density of 300 massive clusters  $\text{kpc}^{-3}$  or an average separation of  $\sim 150$  pc. Note that crowding of clusters in the ring is not an issue for our cluster detection routines and subsequent photometry.

additional shear.

Note that the peak of the cluster MF occurs near  $\log(M_{\text{cl}}/M_{\odot}) = 5.5\text{--}5.6$ , i.e., close to the ‘universal’ peak of the (old) globular cluster MF in the Milky Way and nearby galaxies,  $\log(M_{\text{cl}}/M_{\odot}) \simeq 5.3$ . Stellar evolution of a solar-metallicity SSP from 10 Myr to 10 Gyr will lead to a reduction in mass by  $\sim 35\text{--}40\%$  due to stellar mass loss, i.e., through stellar winds and supernova activity (cf. Leitherer et al. 1999). We thus anticipate that continued cluster disruption, combined with evolutionary mass loss, will result in an even closer match by the time the young ring clusters reach similarly old ages.

The only alternative explanation of the derived lognormal MF is that the high shear in the starburst ring has created an environment in which the formation of low(er)-mass clusters ( $M_{\text{cl}} \lesssim$  a few  $\times 10^4 M_{\odot}$ ) is suppressed, while high-mass clusters are formed more readily. However, this seems contrary to observational results, where more massive star clusters are usually found in environments affected by less shear (e.g., Weidner et al. 2010). On the other hand, Dowell et al. (2008) concluded that “[t]he observed similarity of the initial cluster mass functions in irregular and spiral galaxies implies that the process determining the masses of clusters does not depend on galactic shear” (see also Zhang et al. 2001; Whitmore et al. 2005). We thus conclude that the high shear in the NGC 7742 circumnuclear starburst ring has most likely led to extremely rapid cluster disruption, a view corroborated by the numerical simulations of young clusters in the similarly forbidding environment of the Galactic Center (e.g., Kim et al. 1999; Portegies Zwart et al. 2001). Further supporting (although circumstantial) evidence is found in the MF of the objects in the youngest chimney that are located outside the starburst ring. Although this sample includes only 45 objects, it exhibits a clear power-law MF for  $M_{\text{cl}} \gtrsim 10^5 M_{\odot}$  (i.e., a power law extending to significantly lower masses than for the clusters in the ring, by up to an order of magnitude), indicative of a dynamically younger cluster population.

### Acknowledgements

We thank Doug Lin for useful discussions. This paper is based on archival observations with the NASA/ESA *HST*, obtained from the ST-ECF archive facility. This research has also made use of NASA’s Astrophysics Data System Abstract Service. We acknowledge research support through grant 11073001 from the National Natural Science Foundation of China.

## REFERENCES

- Anders, P., Bissantz, N., Fritze-v. Alvensleben, U., & de Grijs, R. 2004, *MNRAS*, 347, 196
- Barth, A. J., Ho, L. C., Filippenko, A. V., & Sargent, W. L. 1995, *AJ*, 110, 1009
- Bastian, N., Gieles, M., Lamers, H. J. G. L. M., Scheepmaker, R. A., & de Grijs, R. 2005, *A&A*, 431, 905
- Brüns, R. C., Kroupa, P., Fellhauer, M., Metz, M., & Assmann, P. 2011, *A&A*, 529, A138
- Buta, R., Treuthardt, P. M., Byrd, G. G., & Crocker, D. A. 2000, *AJ*, 120, 1289
- Comerón, S., Knapen, J. H., Beckman, J. E., & Shlosman, I. 2008, *A&A*, 478, 403
- de Grijs, R. 1998, *MNRAS*, 299, 595
- de Grijs, R., & Anders, P. 2006, *MNRAS*, 366, 295
- de Grijs, R., & Goodwin, S. P. 2008, *MNRAS*, 383, 1000
- de Grijs, R., Anders, P., Lynds, R., Bastian, N., Lamers, H. J. G. L. M., & O’Neill Jr., E. J. 2003, *MNRAS*, 343, 1285
- de Grijs, R., Anders, P., Lamers, H. J. G. L. M., Bastian, N., Parmentier, G., Sharina, M. E., & Yi, S. 2005, *MNRAS*, 359, 874
- de Grijs, R., Adamo, A., Anders, P., Zackrisson, E., & Östlin, G. 2012, *MNRAS*, submitted
- Dowell, J. D., Buckalew, B. A., & Tan, J. C. 2008, *AJ*, 135, 823
- Fall, S. M., & Chandar, R. 2012, *ApJ*, 752, 96
- Fellhauer, M., & Kroupa, P. 2005, *MNRAS*, 359, 223
- Gieles, M., Bastian, N., Lamers, H. J. G. L. M., & Mout, J. N. 2005, *A&A*, 441, 949
- Ho, L. C. 1997, *Rev. Mex. Astron. Conf.*, 6, 5
- Hsieh, P.-Y., Ho, P. T. P., Kohno, K., Hwang, C.-Y., & Matsushita, S. 2012, *ApJ*, 747, 90
- Kim, S. S., Morris, M., & Lee, H. M. 1999, *ApJ*, 525, 228
- Kotulla, R., Fritze, U., Weilbacher, P., & Anders, P. 2009, *MNRAS*, 396, 462
- Krist, J., & Hook, R. 1997, *The Tiny Tim User’s Guide* (Baltimore: STScI)

- Laine, S., Shlosman, I., Knapen, J. H., & Peletier, R. F. 2002, *ApJ*, 567, 97
- Leitherer, C., Schaerer, D., Goldader, J. D., et al. 1999, *ApJS*, 123, 3
- Maoz, D., Barth, A. J., Sternberg, A., et al. 1996, *AJ*, 111, 2248
- Maoz, D., Barth, A. J., Ho, L. C., Sternberg, A., & Filippenko, A. V. 2001, *AJ*, 121, 3048
- Mazzuca, L. M., Sarzi, M., Knapen, J. H., Veilleux, S., & Swaters, R. 2006, *ApJ*, 649, L79
- Mazzuca, L. M., Knapen, J. H., Veilleux, S., & Regan, M. W. 2008, *ApJS*, 174, 337
- Peletier, R. F., Falcón-Barroso, J., Bacon, R., et al. 2007, *MNRAS*, 379, 445
- Portegies Zwart, S. F., Makino, J., McMillan, S. L. W., & Hut, P. 2001, *ApJ*, 546, L101
- Portegies Zwart, S. F., McMillan, S. L. W., & Gieles, M. 2010, *ARA&A*, 48, 431
- Sarzi, M., Allard, E. L., Knapen, J. H., & Mazzuca, L. M. 2007, *MNRAS*, 380, 949
- Sérsic, J. L., & Pastoriza, M. 1965, *PASP*, 77, 287
- Sérsic, J. L., & Pastoriza, M. 1967, *PASP*, 79, 152
- Sil’chenko, O. K., & Moiseev, A. V. 2006, *AJ*, 131, 1336
- Silva-Villa, E., & Larsen, S. S. 2011, *A&A*, 529, A25
- Tutukov, A. V., & Fedorova, A. V. 2006, *Astron. Rep.*, 50, 785
- van de Ven, G., & Chang, P. 2009, *ApJ*, 697, 619
- Weidner, C., Bonnell, I. A., & Zinnecker, H. 2010, *ApJ*, 724, 1503
- Whitmore, B. C., Gilmore, D., Leitherer, C., et al. 2005, *AJ*, 130, 2104
- Whitmore, B. C., Chandar, R., Schweizer, F., et al. 2010, *AJ*, 140, 75
- Zhang, Q., Fall, S. M., & Whitmore, B. C. 2001, *ApJ*, 561, 727